ISBN: 978-3-95450-233-2 ISSN: 2673-5504 doi:10.18429/JACoW-SRF2021-TUPFDV006

DYNAMICS OF ONE-SIDE MULTIPACTOR ON DIELECTRIC*

Gennady Romanov†, Fermi National Accelerator Laboratory, Batavia, IL, USA

Abstract

Breakdown of dielectric RF windows is an important issue for particle accelerators and high-power RF sources. One of the generally considered reasons for the RF windows failure is the multipactor on dielectric surface. The multipactor may be responsible for excessive heating of dielectric and discharge of charges that accumulated in ceramic due to secondary emission. In this study the comprehensive self-consistent PIC simulations with space charge effect were performed in order to better understand the dynamic of one-side multipactor development and floating potential on dielectric induced by the emission. The important correlations between the multipactor parameters at saturation and the secondary emission properties of dielectric and the applied RF field parameters were found and are reported in the paper.

INTRODUCTION

One side multipactor, which is typical for RF windows, requires a returning force to develop. In case of isolated metal or dielectric body the returning force can be a result of floating potential which is due to charging of the isolated body by emission current. Also, an inhomogeneous RF field can by itself ensure the return of the emitted electrons to the body surface, but this case is not considered here. Buildup in the surface charge starts with random colliding electrons that come from other processes and sources with energy enough to generate larger number of secondary electrons. If the certain conditions are met, then, at early stage of multipactor development, the emission current (the secondary electrons that leave the body) is larger than the collision current (the electrons that return to and hit the body), so the surface charge buildup continues, and positive electric charge is accumulated on the body. With increasing of the returning force more and more of the secondary electrons start to return to the emitting surface and contribute to the floating potential. This stochastic process requires sufficiently high secondary emission yield of material (SEY) to be realized, and, unfortunately, the dielectric materials of RF windows typically have very high secondary emission yield (SEY=8-10 for alumina). Obviously that this charging cannot continue indefinitely and eventually the process comes to saturation at some equilibrium floating potential on dielectric.

The time-dependent physics of the one-side multipactor was studied in detail with self-consistent particle in cell (PIC) numerical simulations using CST Particle Studio. The main advantages of this PIC solver are true multiparticle dynamic, 3D space charge distribution, RF and static fields distortion due to impact from the space charge and the surrounding, advanced secondary emission models. It turned out that besides space charge effect the realistic energy spread of the secondary electrons to a large extent defines the dynamic of this type multipactor.

* Operated by Fermi Research Alliance, LLC under contract No .DE-AC02-07CH11359 with the United States Department of Energy
†gromanov@fnal.gov

Particle-in-Cell Model

The principal PIC model is simple: it is a dielectric plate 40x20x0.2 mm placed in the static and radiofrequency (RF) electric fields. Uniform electrostatic electric field is perpendicular to the plate surface and acts as a returning force in the simulations without space charge effect, and it is disabled in simulations with space charge effects. With space charge effect a returning force is generated by a positive charge accumulated on the dielectric plate. Uniform RF electric field is parallel to the dielectric surface in both cases and provides the electrons with energy for the secondary electron generation. The equations of the electron motion in this case are as follows:

$$m\ddot{y} = -eE_{DC}; \quad m\ddot{x} = -eE_{rf0}\sin(2\pi ft + \theta) \qquad (1)$$

where x and y are respectively horizontal and vertical coordinate of the electron; m – electron mass; e – electron charge; E_{DC} – static electric field (external or induced by MP); E_{rf0} – amplitude of RF electric field; f – frequency of the RF field; θ – phase of the RF field at the moment of electron emission (initial phase of the emitted particle).

The emission property of plate's material is provided by assigned secondary emission model. Because of several reasons it was decided not to use the advanced probabilistic Furman emission model from CST library, and the dielectric plate was provided with the imported Vaughan emission model. The important incident energies of its SEY function are threshold energy W_t (SEY=0 below W_t), first crossover W_1 (SEY=1), W_{max} (SEY is maximal) and second crossover W_2 (SEY=1). The maximums of SEY functions varied from 1.5 to 3, which is much lower than a maximal real emission of dielectrics can be. The SEY was lowered in the simulations to avoid excessive number of particles being tracked and reduce time of simulation.

The only random gamma distributed initial energy of secondary electrons W_0 with maximum of probabilistic density function at 7.5 eV was used in all simulations.

The source of initial particles was placed in the center of the plate. It emitted particles at start of the simulations during one RF period T=1/f to cover all possible initial phases of particles. Total number of initial electrons was typically large ~10^4-10^5 since most of them usually are lost after emission ends without multiplication. For easier interpretation of starting stage of simulation, the initial electrons were monoenergetic with fixed energy of 7.5 eV and did not have angular spread – they all were emitted perpendicularly to the surface. Note, that this setting worked for initial particles only – during further simulations the parameters of secondary electrons were governed by chosen emission model.

ISBN: 978-3-95450-233-2 ISSN: 2673-5504 doi:10.18429/JACoW-SRF2021-TUPFDV006

Simulations without Space Charge Effect

The simulations without space charge effect were performed to evaluate the range of field levels that are favorable for multipactor development. The parameters of the emission model used for the evaluation were: maximal SEY_{max}=1.8 at W_{max}=150 eV, W_t=0, W_1=22 eV and W_2=1147 eV. The analytically estimated threshold fields were E_{RF} = 21.13 kV/m for 325 MHz RF field (the field that accelerates a secondary electron launched at initial phase θ=0° to energy ≥ W_1 during half RF period) and E_{DC}.= 12 kV/m for the electrostatic field (the field provides time of flight equal to half of RF period T/2 for secondary electron with most probable emission energy of 7.5 eV). In the simulations the RF field amplitude was swept from 18 kV/m to 110 kV/m, and the electrostatic field was changed from 7 kV/m to 26 kV/m.

In these simulations without space charge effect the single point particle source was used for clearer picture of emission process. In Fig. 1 the evolution of the emitted beam in the crossed analytically estimated fields during half of RF period is shown. The head of the electron train is emitted at t = 0 and initial phase θ = 0 and hits the plate at t = T/2. The collision energy of the electrons is appropriate to generate a bunch of the secondary electrons, which have now different velocities by values and directions accordingly to the emission model.

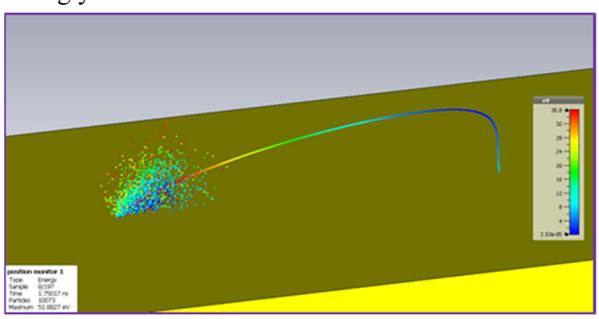

Figure 1: Particle distribution at 1.75 ns after start of emission. The curve before collision is not a particle trajectory, but a continuous chain of particles. After the collision there is a cloud of the secondary electrons with random initial energies and directions.

Further developments of MP simulated at different E_{DC} are shown in Fig. 2. The simulations show that MP starts at 10 kV/m which is less than analytical estimation of 12 kV/m, but on the other hand at higher RF field amplitude of 24 kV/m. At E_{RF} < 24 kV/m MP didn't start at any level of the electrostatic field. Noticeable, that number of particles vs time demonstrates exponential growth and resonance character.

The results of the simulations without space charge effect are not realistic but they help to define the range of parameters and to understand the correlations between them. Electrostatic field of 10 kV/m makes resonant the particles with initial energy

$$W_0 = \frac{m}{2e}\left(\frac{E_{dc}e}{4fm}\right)^2 = 5.2\ eV, \qquad (2)$$

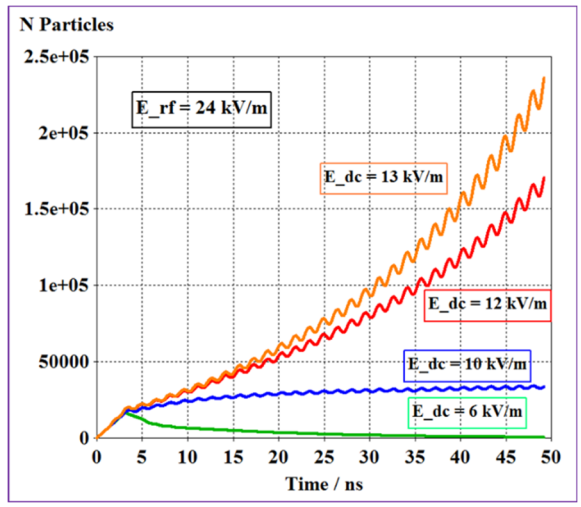

Figure 2: Number of particles vs time at different returning electrostatic field strength and RF field amplitude of 24 kV/m.

which means that the secondary electrons with initial energy 5.2 eV (close to the most probable value of 7.5 eV and therefore the number of initial electrons with this energy is almost maximal according to secondary electrons PDF) are resonant, having time of flight equal to the half of RF period. It is very important to conclude from (2), that there are always the resonance secondary particles emitted with proper initial velocity at any level of electrostatic field, though the number of them after emission is different according to the continuous PDF of initial energies. It should be also noted that the resonant particles with initial energy that exceeds 7.5 eV significantly can exist only with an external fixed electrostatic field. If too high E_{dc} makes secondary electrons with energies above 7.5 eV resonant, then the number of emitted resonant particles drops according to the given PDF. The electrostatic field, which is due to the charge induced by emission, decreases with the lowered emission current, and the resonance returns to the particles with initial energy ≤7.5 eV. An autoregulation of positive charge on the ceramic in the similar practical case is also described in [1].

Evaluation of the breakdown level of RF field for very low electrostatic field made in [2] assumes only non-resonant motion of the electrons (so called polyphase regime: time of flight τ >> T for all electrons, collision phases are uniformly distributed over RF period). This approach is correct for low electrostatic fields since the number of resonant electrons with very low initial energy is negligibly small. For the considered emission parameters W_1 = 22 eV and f=325 MHz the breakdown level following [2] is

$$E_{rf\_breakdown} = 0.94 \cdot 2\pi f\sqrt{\frac{2U_1 m}{e}} = 30.4\frac{kV}{m}, \qquad (3)$$

where U_1 = W_1/e = 22 V is the first crossover potential. The breakdown level of E_{RF} obtained in the simulations is much lower (24 kV/m), which suggests a contribution from more effective and faster resonant multipacting to the growth of particle number in time.

ISBN: 978-3-95450-233-2 ISSN: 2673-5504 doi:10.18429/JACoW-SRF2021-TUPFDV006

SPACE CHARGE EFFECT

Saturation

The main impact of the space charge on virtually all kinds of multipactor is a saturation of the multipactor. In case of RF electric field parallel to dielectric surface the saturation of the discharge is combined with the saturation of the charge accumulated in dielectric. To study this time dependent process the PIC simulations were performed with active space charge effect.

For simulations with space charge effect the model was modified. The external electrostatic field was removed, a voltage monitor was added at the bottom of dielectric plate away from multipactor area. The single point particle source was replaced with a circular one to make an initial charging of the ceramic more uniform. Total charge emitted during one RF period was chosen equal to 1e-9 C. Vaughan emission model parameters were W_t=0, W_1=11 eV, maximal SEY of 3.0 at W_{max}=200 eV and W_2=6470 eV.

Initial emission from particle source instantly generates a potential on the dielectric surface, so there was no need to use any ancillary electrostatic field, which was used in some models to initiate multipactor process [3]. Particle distribution in space after 2 ns of emission is shown in Fig. 9. Some particles leave the dielectric along straight trajectories. Apparently, they are the very first particles emitted when the electrostatic field is not enough yet to return them to the surface. Gradually the emitting electrons build up a positive charge on the dielectric and the particles start to return to the surface.

Development of MP at different levels of RF field during simulation time of 15 RF periods is shown in Fig. 3. Breakdown level of E_{RF} is about 25 kV/m, which is slightly lower that was found in the simulations without space charge effect with external electrostatic field. Further increasing of RF field above the breakdown level changes the speed of MP development, but the saturation level of number of particles remains almost the same at each RF field value, it just slightly increases in average.

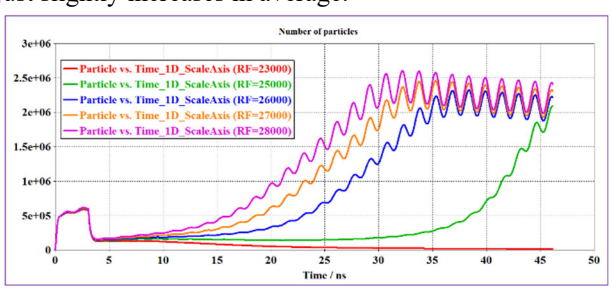

Figure 3: Number of particles vs time at different levels of RF field.

The electrostatic field induced by MP at the end of simulation is not uniform, and its distribution depends also on the surrounding. The voltage monitor of the electrostatic field was located under the plate and integrated electrostatic field along 2 mm line perpendicular to the plate. The location has been chosen to avoid interference of the monitor with the space charge of the particle cloud. The field strength is obviously different above and below the plate, so the monitor readings are relative. The voltage monitor in Fig. 4 also shows some dependence of the saturated electrostatic field level as well as growth rate on the applied RF field. Qualitatively the curves in Fig. 4 are in a good agreement with experimental measurements of the potential on the stainless-steel target at different RF power levels as function of time ([2], see Fig. 32].

The collision energy vs time also saturates in the similar fashion as other MP parameters (see Fig. 5). But there is one more important feature in addition to the dependence of the collision energy on the applied RF field. Namely, the phase of collision also depends on the applied RF field strength, which is shown clearly in the insert of Fig. 5. This dependence will be discussed later.

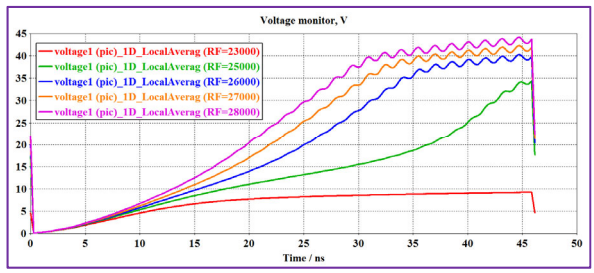

Figure 4: Data from voltage monitor for different RF field levels.

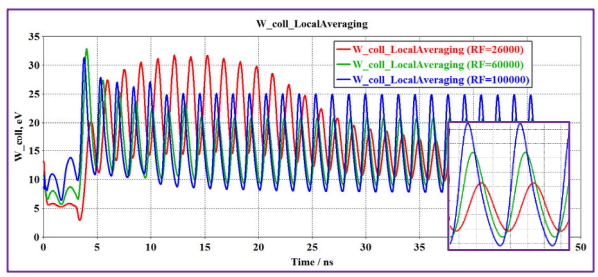

Figure 5: Collision energy vs time for different RF field levels. The insert shows the shift of collision phase with increasing of RF field level

Impact of the Emission Model Parameters

Four different SEY functions were used to investigate impact of SEY on multipactor dynamic. Their parameters are shown in the Table 1. The initial energy distribution of the secondary particles was the same in all simulations.

Among the emission model parameters, the first crossover W_1 of the SEY function plays especially important role in the MP process. It defines RF field level at which multipactor begins (threshold) and influences the saturation levels of multipactor parameters. Figures 6 and 7 show the set of collision currents and collision energies for different first crossovers vs RF amplitude.

Table 1: Parameters of Four SEY Functions

SEY_{max}	W_{max}, eV	W_1, eV	W_2, keV
3	200	11	6.6
3	200	16	6.5
1.8	150	22	1.1
3	220	31	7.0

ISBN: 978-3-95450-233-2 ISSN: 2673-5504 doi:10.18429/JACoW-SRF2021-TUPFDV006

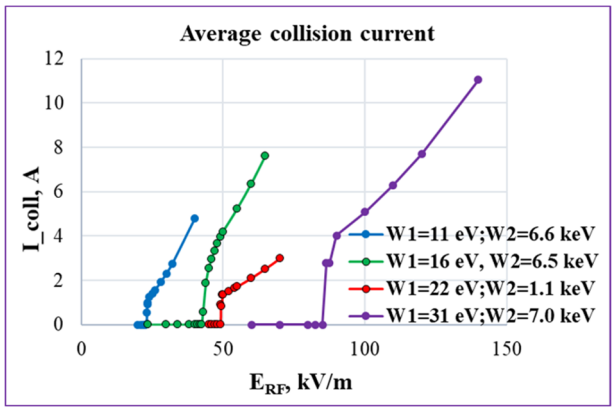

Figure 6: The collision currents vs RF field amplitude for different crossovers W_1 and W_2.

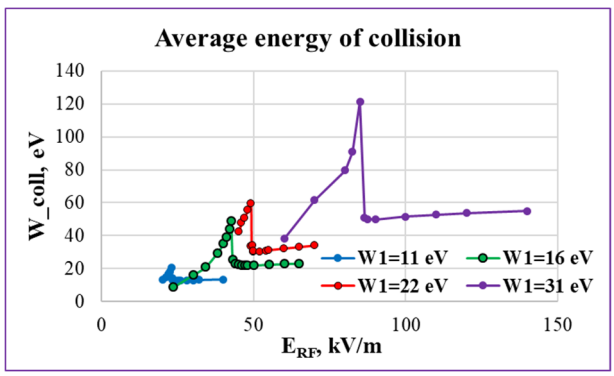

Figure 7: The collision energies vs RF field amplitude for different first crossovers W_1.

The RF field thresholds and the saturated energies of collision obviously depend on the first crossover W_1. Apparently, the growth rates of the collision currents are correlated with second crossover W_2. Both the threshold RF field amplitude and the collision energy at the thresholds are linear functions of first crossover W_1 as shown in Fig. 8. The theoretical prediction of threshold made with formula (2) is also shown to compare with. There is a disagreement between the theory and the simulations, and it increases dramatically with increasing of W_1. The theory assumes a polyphase regime at low E_{DC}, and it assumes also that it remains polyphase. But the voltage (i.e. E_{DC}) sharply jumps to much higher level at threshold (Fig. 9). It means that the electrons with higher initial energy W_0 and therefore more numerous become resonant, so the overall MP process becomes dominantly resonant.

The DC voltage shown in Fig 9 is relative as it has been mentioned earlier, because it is measured on the plate side without MP, but we can make some qualitative speculations about surface charge at saturation.

Under assumption that the resonance MP dominates at saturation, the initial energy of resonant secondary electrons is one of the factors that regulates charging of dielectric. The number of resonant electrons among the secondaries should be high enough to support multipacting. In other words, the resonant electrons must have an initial energy hovering around W_{max} of PDF. In simplified picture without considering other factors, if E_{DC} increases and exceeds the level, above which the secondary electrons with initial energy higher than W_{max} become resonant, then the number of such resonant particles goes down, a dielectric discharges and E_{DC} returns to some equilibrium level.

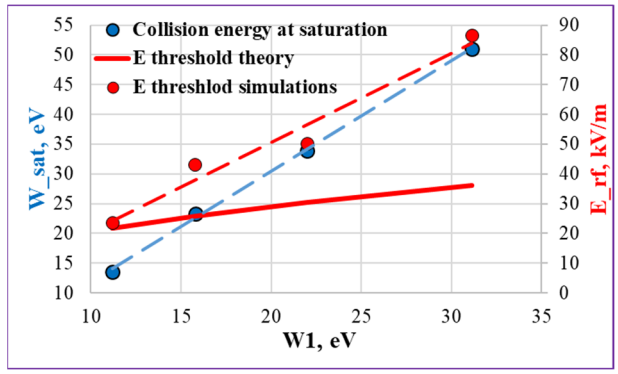

Figure 8: RF field threshold and average collision energy at saturation vs first crossover of SEY. The threshold according to theory [2], which assumes completely polyphase regime, is given for comparison.

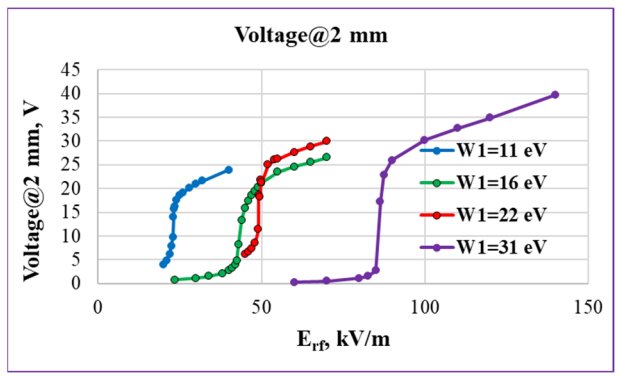

Figure 9: The voltage monitor readings vs RF field amplitude and different first crossovers of SEY functions.

Figure 10 shows the charging of dielectric plate that develops synchronously with increase and saturation of the collision current. The insert in the right corner of the figure shows almost uniform distribution of the collision current over time at low levels of electrostatic field in the beginning of MP development. This confirms the speculation that MP on a dielectric starts in a polyphase (non-resonant) regime, which gradually transforms to a dominantly resonance process as the charge on the dielectric increases.

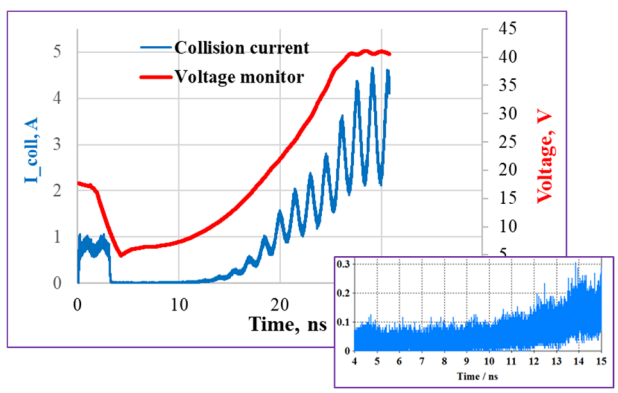

Figure 10: Transition of multipactor development from the polyphase regime to the resonance one.

ISBN: 978-3-95450-233-2 ISSN: 2673-5504 doi:10.18429/JACoW-SRF2021-TUPFDV006

The fact that the collision energy at saturation almost does not depend on RF field level can be explained by a variation of initial phase of resonant particle. Figure 11 shows the evaluation of the average initial phases that provide different fixed energy of collision based on the simulations and compared to the analytical calculations of the same energy for resonant particle (time of flight is T/2) and variable initial phase made with equations (1).

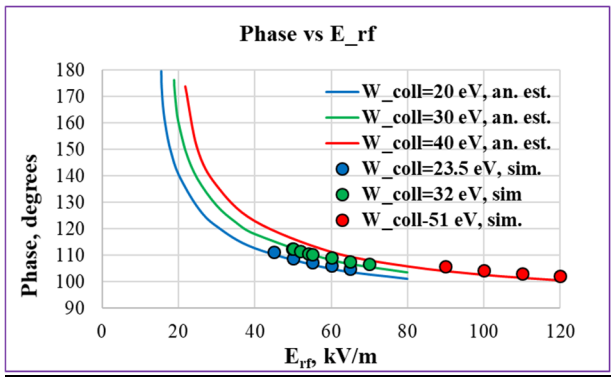

Figure 11: Average initial phase θ of the resonant electrons that provides certain W_{coll} vs E_{RF}. The phases calculated from the simulations are compared to the analytical calculations made with equations (1).

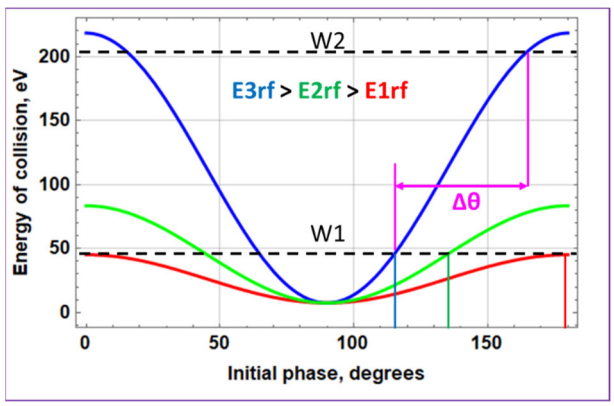

Figure 12: Analytical evaluation of the resonant particles' energy of collision as a function of initial phase at different amplitudes of RF field. The crossover energies W_1 and W_2 are arbitrary and serve for qualitative explanation of the initial phase variation.

Figure 12 illustrates the mechanism of the initial phase variation of the resonant particles. The solid lines are energy of collision of the resonant particles vs their initial phases at given level of RF field. The collision energies of the particles were calculated using equations (1). The behaviour of the energy of collision vs RF field level is explained by the fact that a resonant particle is accelerated during part of time of flight and deaccelerated during the rest part of flight, excluding initial phases 0° and 180° at which an electron is accelerated in one direction full half of RF period. Therefore, the energy of collision is a difference between acquired and lost energies. The dashed lines are the crossover energies W_1 and W_2 of SEY, their levels are arbitrary and chosen to fit the plot conveniently. Formally MP starts at RF field level of $E1_{RF}$ and its initial phase of 180°, once the energy of collision reaches first crossover W_1 (the phases 90-180° were chosen for the speculations because in this interval auto phasing and phase stability are expected). From this point of view, it is clear why the RF field level at which MP starts depends on W_1. The MP starts when the range of appropriate initial phases Δθ is big enough to develop multipacting process, say at field level $E2_{RF}$. The multipactor continues with RF field increase as long as Δθ stays sufficiently big. With further RF field increasing the Δθ starts shrinking, and MP should stop when Δθ gets lower some critical value, though that level of RF field was not reached in the simulations due to numerical challenges.

SUMMARY

This work is to summarize the results of PIC simulations of one-side multipactor on dielectric and to accumulate the observations of the features of the process, some of which are not understood in full yet. Therefore, the following list of the observations is rather a list of suppositions that require further study and verifications than conclusive statements.

- At any DC field there are always synchronous secondary electrons with time of flight T/2 due to continuous distribution of initial velocities given by PDF.
- There are two stage of MP development: 1) dominantly polyphase regime in the beginning of MP and 2) dominantly resonant regime at saturation.
- At saturation E_{DC} and W_{coll} vs E_{RF} are approximately constant for given SEY. The crossovers are important defining parameters for their levels, especially W_1.
- MP dynamic at saturation has tendency to establish average energy of collision W_{coll} close to the first crossover W_1 of SEY.
- MP dynamic via synchronous phase keeps average energy of collision W_{coll} constant while field E_{RF} is varying.
- The horizontal and vertical movements appear to be independent according to the uncoupled equations (1). But the same charge simultaneously affects induced electrostatic field E_{DC} and produces phase-dispersing effect in horizontal direction [4]. Presumably, the space charge in some form couples both equations (1).

REFERENCES

[1] I. Gonin *et al.*, "A Study of Multipactor Phenomena in the 52 MHz PETRA II Cavity at DESY", in *Proc. EPAC'94*, London, Great Britain, June-July 1994, pp. 2197-2199.

[2] L.V. Grishin *et al.*, "Investigation of the secondary emission microwave discharge at large angles of flight of electrons", Proc. of the Physics Institute, Lebedev, vol. 92, pp. 82-131, 1977 (in Russian).

[3] Lay-Kee Ang *et al.*, "Power Deposited on a Dielectric by Multipactor", *IEEE Trans. Plasma Sci.*, vol. 26, no. 3, pp. 290-295, June 1998. doi:10.1109/27.700756

[4] J.R.M. Vaughan, "Multipactor", *IEEE Trans. Electron Devices*, vol. 35, no. 7, pp. 1172-1180, July 1988. doi:10.1109/16.3387